Status of the CLIC Studies on Water Induced Quadrupole Vibrations

R.W. Aßmann, W. Coosemans, S. Redaelli*, W. Schnell, CERN, Geneva, Switzerland

Abstract

Performance of future linear colliders will be limited by vibration of the focusing quadrupoles. The Compact LInear Collider (CLIC) base line includes resistive quadrupoles. They incorporate water cooling circuits, which will increase the vibration level of the quadrupoles. In this paper, the CLIC studies on water induced magnet vibrations are summarized. Theoretical understanding of the phenomenon and detailed measurements on magnet prototypes are presented.

1 INTRODUCTION

Stabilization issues are one of the main concerns for the new generation of high energy linear colliders. Very tight tolerances on the quadrupole vibrations are imposed to maintain the beams in collision and to limit emittance growth. For instance, the uncorrelated RMS motion above 4 Hz of the linac quadrupoles of the Compact LInear Collider (CLIC) [1] must be smaller than 1.3 nm (vertical) and 14 nm (horizontal) [2]. There are places at CERN (like for instance the underground LEP tunnel [4]) where the floor is quiet enough to fulfill these tight tolerances. However, in an accelerator environment these quiet conditions are perturbed by the equipment in the vicinity of the beam. An example is given by the water used to cool the focusing quadrupoles. If the cooling circuit is not properly designed, water induced vibrations can increase the quadrupole motion to an unacceptable level. In the framework of the CLIC Stability Study, measurements have been done to quantify this effect for the quadrupoles of the CLIC Test Facility II (CTF2) [3], which have a similar design to the ones foreseen for the CLIC linac. In this paper the theoretical understanding of water induced vibrations and the results of quadrupole vibration measurements are summarized.

In Section 2 a simple theory of the water induced pipe vibrations is developed. To estimate the frequency range and amplitude of the vibrations induced by water in turbulent regime, the approach of [6] and the results of [7] are used. In Section 3 the experimental setup for vibration measurements is presented. The measurement results, as obtained with different stabilization devices, are summarized in Section 4. In Section 5 some in-situ measurements performed in the CTF2 site are given. Conclusions are drawn in Section 6.

* PhD student of the University of Lausanne, Institut de Physique des Hautes Energies (IPHE), Switzerland.

2 SIMPLE THEORY OF WATER INDUCED PIPE VIBRATIONS

Consider a straight pipe with diameter d, with water circulating at a velocity u. For laminar motion, no vibration should be generated since the water velocity at the internal pipe wall is zero. Turbulence in the water motion will instead transmit additional vibration to the pipe. Turbulence onset depends on the values of the Reynold's number, defined as

$$Re = \frac{ud\rho}{\eta}, \tag{1}$$

where u is the water velocity, d the pipe diameter, ρ=10^3 kg m^{-3} and η=$0.89\,10^{-3}$ kg m^{-1} s^{-1} the water density and dynamic viscosity. For given pipe geometry and cooling fluid, the Reynold's number depends only on the fluid velocity u. Turbulence occurs when the Reynold's number reaches a critical value Re_{cr}, which depends for instance on the roughness of the pipe surface, on the pipe shape and on the status of the water upstream of the pipe. A typical values is $Re_{cr} \approx 2000$. In the following, the water motion will be assumed to be laminar upstream and downstream of the pipe under consideration, i.e. other water induced vibrations than the ones induced by the pipe itself are neglected.

In the turbulent regime, an eddy-like motion is superimposed to the drift of the water. Domains of coherent eddy motion appear above turbulence and drift with velocity u. These domains induce a modulation of the water motion with a frequency that depends on their size. This is shown in Fig. 1. The local rotation velocity of the eddies in a frame moving with the water (v_λ) depends on the eddy size (λ) as $v_\lambda \sim \Delta u(\lambda/d)^{3/4}$, where Δu is the velocity of the largest eddies and can be of the order of the water velocity u (see [7] for more details). The largest domains have a typical size of the order of the pipe radius i.e. $d/2$. For too small values of v_λ, locally the motion can go below the turbulence limit. This occurs for local velocities cor-

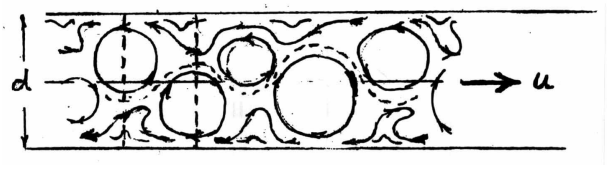

Figure 1: In the turbulent regime, an eddy-like motion is superimposed to the drift of the water. Coherence motion domains drift with velocity u. They induce a modulation to the water motion whose wave length is roughly twice the eddy diameter.

responding to Reynold's number smaller then the critical value of Eq. (1), i.e. $v_\lambda \lambda \sim ud$. This condition determines the smallest size of the eddies, which can be estimated from the above scaling low as $d/Re^{3/4}$.

The largest domains fix a lower value of the turbulence induced vibration frequency as

$$f_{\min} = \frac{u}{d}, \tag{2}$$

which is a frequency associated to coherence domains of length equal to the tube radius. On the other hand, the smallest eddies fix the largest vibration frequency as

$$f_{\max} = \frac{u}{d} Re^{3/4}. \tag{3}$$

This value is intended to give only the order of magnitude of the expected frequency range of water induced vibration.

Following the approach of [6] it is possible to estimate the amplitude of the turbulence induced pipe vibrations. In the turbulent regime, the pressure drop along the pipe depends on u^2 as

$$\Delta p = \frac{\rho u^2}{2d} l\lambda, \tag{4}$$

where l is the pipe length and $\lambda \approx 0.316 Re^{-1/4}$=0.04 is an empirical parameter (see, for instance, [8]). In turbulence, the hydrostatic energy density is converted into kinetic energy density. If the pump power is *completely* converted in irretrievable kinetic energy, i.e. $\frac{\partial V}{\partial t}\Delta p = \frac{\partial V}{\partial t}\rho\frac{\overline{v^2}}{2}$, then the pressure drop Δp is given by:

$$\Delta p = \frac{1}{2}\,\rho\,\overline{v^2}. \tag{5}$$

Here, $\overline{v^2}$ is the mean square velocity of turbulence seen from a frame moving with velocity of the water, u.

The fluid can be divided in coherence cells of mean velocity $\overline{v^2}$. In the approximation of isotropy of the turbulence, i.e. $\overline{v_y^2} = \overline{v^2}/3$ (y denotes the, say, vertical direction), Eqs. (4) and (5) give the following expression for the RMS vertical vibration velocity of one coherence cell:

$$v_y^{\text{RMS}} = u\sqrt{\frac{\lambda l}{3d}}. \tag{6}$$

The local momentum density of one cell is ρv_y^{RMS}. In order to calculated the total kinetic energy released to the pipe, some assumptions on the volume over which the energy is released have to be made. It seems reasonable (and somehow pessimistic) to assume the kinetic energy to be concentrated in cells of the same size as the coherence domains, i.e. $d/2$. The contributions from the different cells are assumed to be uncorrelated and must be added in quadrature. The total momentum transferred to the water is then

$$P_{y,\text{Tot}}^{\text{RMS}} = \sqrt{\frac{2l}{d}}\frac{\pi d^3 \rho}{2} v_y^{\text{RMS}} = mu\sqrt{\frac{\lambda}{6}}, \tag{7}$$

where m is the mass of the water in the pipe. The coefficient $\sqrt{2l/d}$ is the square root of the cell number and comes from the sum in quadrature. $\pi d^3\rho/2$ is the mass of the water in one cell. If the pipe itself does not have internal resonances and can be considered as a rigid body of total mass M, i.e. $P_{y,\text{Tot}}^{\text{RMS}} = M v_{y,\text{Tot}}^{\text{RMS}}$, its velocity is

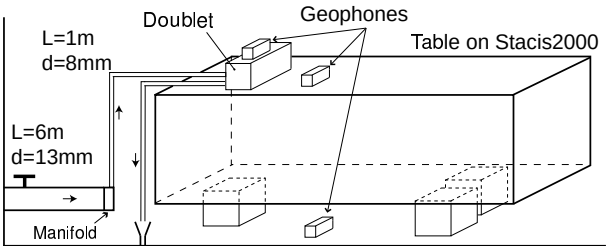

Figure 2: Scheme of quadrupole and geophone installation and of the connection to the water tap.

$$v_{y,\text{Tot}}^{\text{RMS}} = \frac{m}{M} u\sqrt{\frac{\lambda}{6}}. \tag{8}$$

For a pure harmonic oscillation at the frequency f_0, the RMS amplitude corresponding to the RMS velocity of Eq. (8) would be $v_{y,\text{Tot}}^{\text{RMS}}/(2\pi f_0)$. In the pessimistic assumption that all the energy is concentrated at the minimal vibration frequency $f_{\min} = u/d$, the vertical RMS vibration amplitude of the pipe becomes

$$y_{\text{Tot}}^{\text{RMS}} = \frac{1}{2\pi}\frac{m}{M} d\sqrt{\frac{\lambda}{6}}. \tag{9}$$

Surprisingly, the vibration amplitude does not depend directly on the water velocity, there is only a small dependence as $u^{-1/8}$ due to the λ dependence on Re. The agreement of this result with the experimental data will be discussed in the Sections 4.

3 EXPERIMENTAL SET-UP

A scheme of the experimental setup and a photo showing details of sensor and quadrupole installation are given in Figs. 2 and 3, respectively. A CTF2 quadrupole doublet was directly screwed on top of a honeycomb table, which was supported by actively stabilized feet [2, 9]. The systems utilized are able to damp efficiently the vibration level of the floor, so providing a very low background noise. This quiet condition is suitable to study the pure effect of the water motion on the quadrupole vibrations.

The cross section of the CTF2 quadrupole [5] used in the measurements, with its transverse dimensions, are given in Fig. 4. Each quadrupole is 80 mm long, weight 6.7 kg and has four copper coils made of six rectangular conductors, with a 3 mm diameter hole for the cooling water to circulate. The CLIC quadrupoles will have the same cross section but will be longer. Each quadrupole has one feeding channel. Two magnets forming a doublet sit on a common support plate and have independent water connections. The doublet used in our measurements was connected to the regular Geneva tap water system (pressure of about 4 bar).

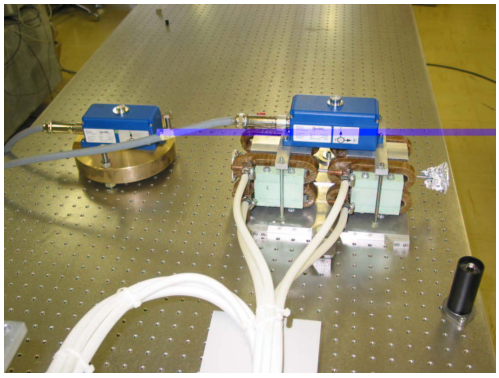

Figure 3: Detail of the installation of the doublet used for the measurements. The doublet is fixed on top of the honeycomb table described in [9], which is mounted on a stabilization device. The white cables feed the cooling circuit inside the magnet coils.

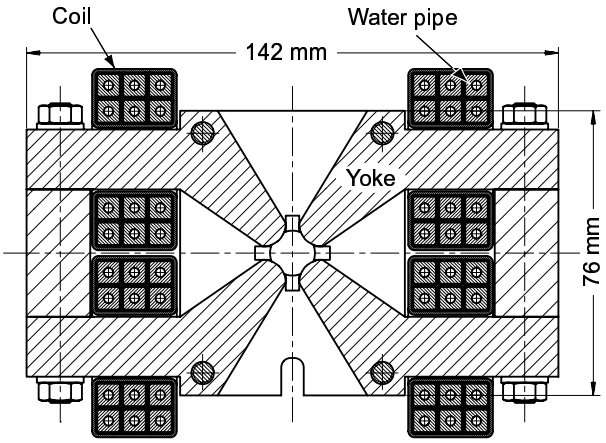

Figure 4: Cross section of the CTF2 quadrupole with its transverse dimensions [5]. The cross section is the same as CLIC quadrupoles, which will be longer.

It was not possible to connect it to pumped demineralized water, like in operational conditions.

Fig. 2 shows schematically how the quadrupoles were connected to the tap. Three different pipes were used. The water was first brought from the tap to a 4 channel manifold and then to the quadrupoles with tubes of different diameter. In Table 1, the minimal flows required for the turbulence onset and the corresponding minimal vibration frequencies of Eq. (2) are listed for all kinds of pipes of interest. The maximum turbulent frequency, according to Eq. (3), is given by $Re^{3/4} f_{\min}$ and is well above the maximal frequency of the geophones used for the vibration measurements (315 Hz). The water volume rate was measured with a precision of 1%. The maximum water velocity in quadrupole pipes was of about $3\,\mathrm{m\,s^{-1}}$ (the nominal value for the CTF2 quadrupoles is $1.2\,\mathrm{m\,s^{-1}}$ [5]).

Three triaxial geophones of the type described in [2] (~ 1 Hz to 315 Hz frequency range) were fixed on top of the doublet, on the table and on the floor. Geophones provide a measure of the mechanical vibration velocity versus time. The power spectral density of the displacements as a function of frequency, $P(f)$, is calculated from the Fourier transform of the velocity. The RMS motion above a given frequency f_0 is then obtained from the integral of $P(f)$ from f_0 to 315 Hz. The measurements were taken over night, to have the quietest background conditions. Data were acquired with a sampling time of 0.001 s for about 3 minutes and the results were averaged over subsamples of 5 s.

Table 1: Diameter of the different pipes on interest, flow required for the turbulent onset and minimal vibration frequency according to Eq. (2).

Pipe	Re	d [m]	Flow [l/h]	$f_{\min}$ [Hz]
Tap→Manifold	2000	0.013	16.4	10.5
Manif.→Quad	2000	0.008	40.3	27.9
Quadrupole	2000	0.003	15.1	198

Quadrupole vibrations were measured with different stabilization devices. The system shown in Fig. 3 was tested with three or four stabilizing feet. This is a stiff system that features a rubber layer to provide passive damping of the floor motion and damps the residual vibrations by means of piezoelectric actuators. In addition, also a soft air pressure system was used. In the next section, the results of these measurements are analyzed. More details on these devices can be found in [2] and in these proceedings [9].

4 RESULTS OF THE MEASUREMENTS

4.1 Measurements on a Stiff Stabilization System with Three Feet

In Fig. 5 the power spectral densities of the vertical quadrupole displacements are given for different values of water flow. The peaks of the zero flow line are mostly induced by floor motion, damped by a factor between 10 and 100 by the stabilizing support [2]. Fig. 5 shows that the turbulence is a threshold phenomenon. Effects of water induced vibrations are found only for flows larger than 15 l/h. In fact, the 12.5 l/h flow line in Fig. 5 is completely superimposed to the zero flow line. This is good agreement with what is to be expected from Table 1. The pipe from the tap to the manifold and the pipe of the quadrupoles themselves are the possible candidates for the turbulence to occur. The pipes from the manifold to the quadrupole is expected to have an effect for flows above 40 l/h.

Typical power spectral densities of vertical displacements of the doublet for different water flows are given in Figs. 6 and 7. Arbitrarily, data have been divided in two different frequency ranges. Above the turbulence threshold, two main effects induced by the circulating water are observed. (1) The released energy increases the overall noise level of the quadrupole vibrations. The existing peaks

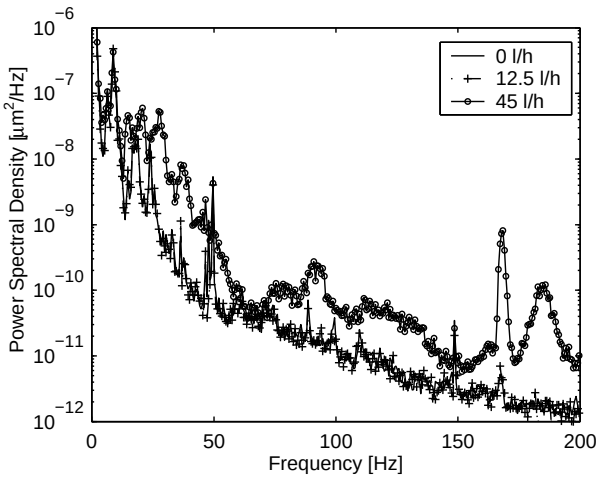

Figure 5: Power spectral density of vertical displacements vs. frequency as measured on top of the CLIC prototype doublet mounted on the stabilized table (see Fig. 2). The 12.5 l/h line is superimposed to the zero flow line. Turbulence effects appear only above 15 l/h.

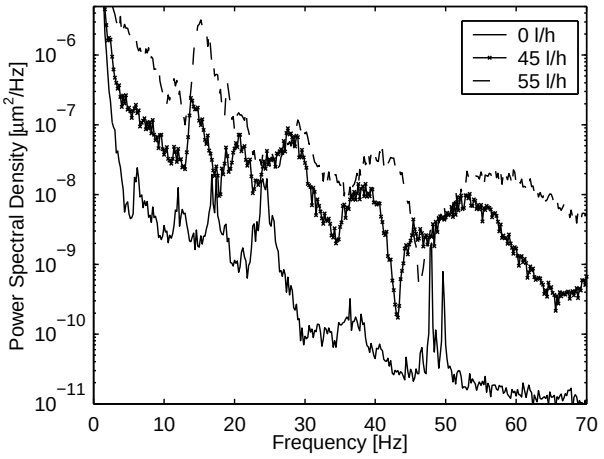

Figure 6: Low frequency content of the water induced vibration. The power spectral density of vertical displacements vs. frequency as measured on top of the CLIC prototype doublet is shown.

of the power spectral density get considerably amplified. This is for instance the case of the noise below 10 Hz and for the peak at around 170 Hz (see also Fig. 5). (2) A number of new peaks arise, which are not present without turbulence. This is the case for a strong peak at 15 Hz (appearing above 45 l/h) and for broad peaks in the 25-45 Hz frequency range (see Fig. 6). In the higher frequency range these two features are even more remarkable: amplifications of the zero flow vibration level of up to 1000 and more are clearly shown in Fig. 7. Three new peaks appear at $\approx$ 90 Hz, $\approx$ 180 Hz and $\approx$ 270 Hz, both in vertical and horizontal directions, whose amplitudes increase for increasing water flows. However, the vibrations above 60 Hz contribute less than 0.2 nm to the total integrated motion (see below).

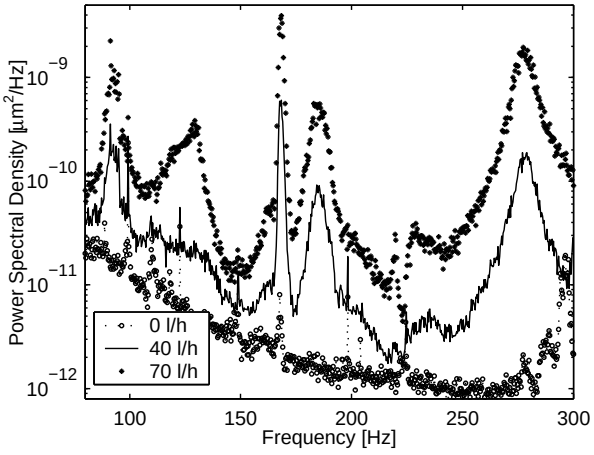

Figure 7: High frequency content of the water induced vibration. The power spectral density of vertical displacements vs. frequency as measured on top of the CLIC prototype doublet is shown.

Fig. 6 shows that the new peaks appearing above turbulence shift with increasing water flows. This is a nice result in qualitative agreement with the theory of Section 2, which foresees that the spectrum of turbulence induced vibrations increases with the water velocity (see Eqs. (2) and (3). On the other hand, this feature is not found for the peaks of Fig. 7, which only increase their amplitude for larger water flows.

In Table, 2 some absolute values of the integrated vertical RMS motion of the doublet above 4 Hz, 20 Hz and 60 Hz are given. The vibration level of the floor is also shown. For the CTF2 operational water flow of 30 l/h, the vertical RMS motion above 4 Hz is 1.3 nm, which meets the limit tolerance for CLIC [2]. Similar values are found for the horizontal displacement, where the tolerance is less demanding. The pure effect of the water is given by the difference in quadrature of the cases with and without flow. Above 4 Hz we obtain 0.9 nm, which is comparable to the theoretical estimate assuming that the doublet and the table move as a whole. Regardless of the theory prediction, the water induced motion is strongly dependent on the water flow. In Fig. 8 we show vibrations versus water flow for different minimal frequencies. We find a maximum vibration level for a flow of around 60 l/h. Interestingly, the vibration levels are lower at even higher water flows. The maximum increase of the quadrupole motion above 4 Hz due to the water is of the order of 3 nm. Note that the contribution of the vibrations above 60 Hz are less than 0.2 nm.

The small motion which is measured above 60 Hz suggests that the the water induced vibrations of the doublet are mainly driven by the turbulence in the upstream pipes (that feed the quadrupoles) rather than in the magnet pipes themselves. From the theoretical estimates it seems unlikely that the small quadrupole pipe can induce vibration at low frequencies (see Table 1). Vibrations are generated in the larger pipe coming from the tap and then transmitted

Table 2: Integrated RMS displacements above 4 Hz, 20 Hz and 60 Hz on floor, on doublet rigidly clamped to a 700 kg table, for zero and operational water flow.

Vertical displacements			
f	Floor	Doublet 0 l/h	Doublet 30 l/h
4 Hz	3.62 nm	0.92 nm	1.30 nm
20 Hz	1.29 nm	0.21 nm	0.74 nm
60 Hz	0.07 nm	0.05 nm	0.06 nm
Horizontal displacements			
4 Hz	2.33 nm	0.35 nm	1.33 nm
20 Hz	0.43 nm	0.18 nm	0.80 nm
60 Hz	0.04 nm	0.04 nm	0.17 nm

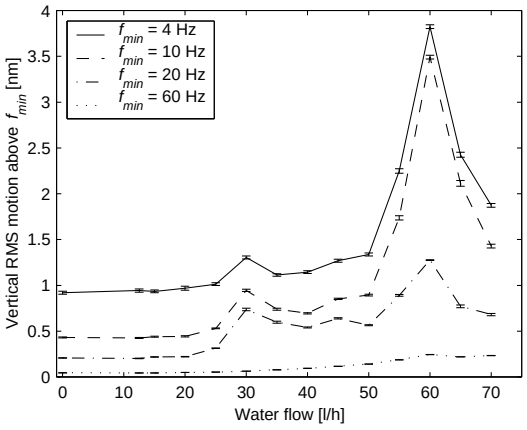

Figure 8: Vertical RMS motion above 4 Hz, 10 Hz, 20 Hz and 60 Hz vs. water flow.

downstream via the pipe or via the water. This feature was also confirmed in measurement done at SLAC [10].

Vibration measurements of a doublet mounted on its CTF2-like alignment support, which was fixed on the stabilized table, have also been performed. The preliminary results show that the horizontal RMS motion above 4 Hz can be amplified by a factor of 2 and more. A support internal resonance at 37 Hz [2] is considerably amplified by turbulence and is the main contribution to the increased motion. The vertical direction is not much affected by the alignment support, as also confirmed by in-situ measurements of the CTF2 quadrupoles.

4.2 Measurements on Soft Stabilization Systems

Vibration measurements were also taken on a soft stabilization device, described in a companion paper [9]. The honeycomb table of Fig. 3 was lifted by air pressure flowing from four feet and providing a very good passive isolation above few Hz. This system has a proper resonance at about 1 Hz. Three geophones measure the vibrations on top of the table and are used as input of a feedback designed to damp the proper resonance (active damping is obtained by

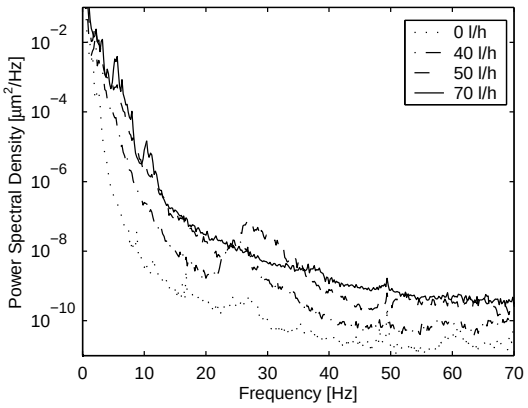

Figure 9: Power spectral density of vertical displacement as measured on the doublet mounted on the air pressure stabilization system.

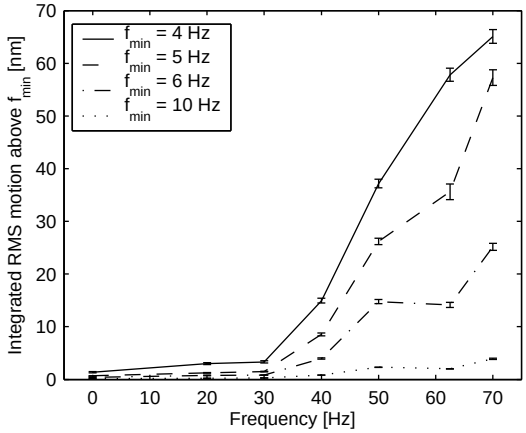

Figure 10: Vertical RMS motion of the doublet when mounted on the air pressure system. Different water flows are shown.

adjusting the air flows). These feedback should not affect much the vibration at frequencies larger than a few Hz.

The power spectral densities versus frequency for different water flows are shown in Fig. 9. The integrated motion versus water flow is given in Fig. 10. With this stabilization system, much larger displacements are measured. The integrated motion above 4 Hz is increasing monotonically for increasing water flows. At 60 l/h, an RMS motion of about 65 nm was measured. However, the motion at the nominal water flow (30 l/h) is about 3.3 nm. These larger displacements are mainly induced by the low frequency content of the vibrations, say up to 10 Hz. Above this frequency, the same features as with the stiff systems are found. For instance, Fig. 9 shows one peaks at about 25 Hz that moves for increasing water flows and eventually disappears. This behavior in the 20 Hz to 40 Hz frequency range was inducing the non-monotonic curves of Fig 8.

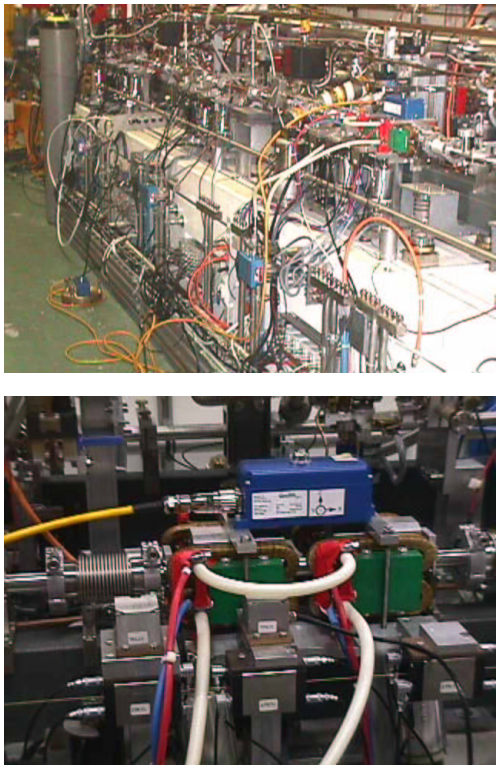

Figure 11: Sensor installation for the in-situ measurements of quadrupole vibrations in the CTF2 site.

5 IN-SITU MEASUREMENT OF THE CTF2 QUADRUPOLES

Quadrupole vibrations were also measured in the CTF2 site. Doublets are mounted on a movable structure for the alignment like the one of Fig. 3, which sits on a concrete block directly glued on the floor basement. The sensor installation is shown in Fig. 11. The CTF2 site is close to streets and measurements were done under particularly noisy conditions (ongoing work in a close by street). This explains the larger vibration level of the floor (15 nm above 4 Hz). Measurements were taken without beam, but with all electronic instrumentation on. Quadrupole coils were not powered but it was possible to switch on and off the cooling water, at the operational flow.

In Figs. 12 and 13 the vertical and horizontal RMS motion of a quadrupole doublet is shown. Measurements on the floor and on top of the quadrupole, with and without circulating water, are shown. The measured vertical and horizontal motion above 4 Hz are 15 nm and 27 nm, respectively. This is well above the CLIC tolerances. The vibration level is larger than the CLIC tolerances, already in absence of circulating water. However, it should be noted that (1) on top of the quadrupole there is basically no amplification of the vertical motion with respect to the floor level and (2) the effect of the water is moderately small (some relevant differences arise only above 50 Hz). Therefore, the large measured motion seems to be induced by the unusually high noise of the ground. It should be checked

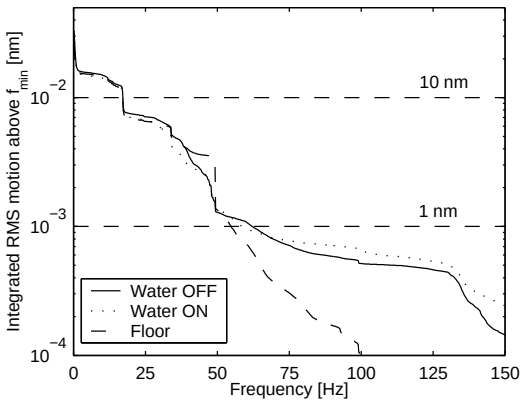

Figure 12: Vertical integrated RMS motion above $f_{\min}$ as measured on top of a CTF2 doublet.

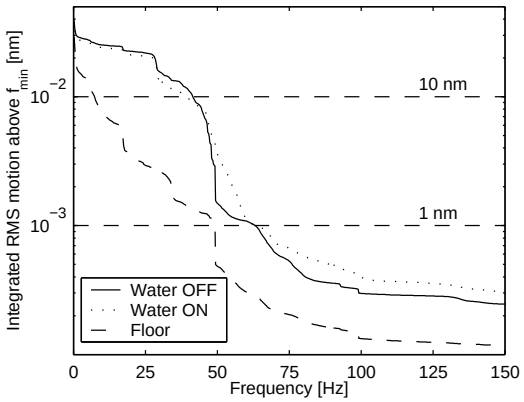

Figure 13: Horizontal integrated RMS motion above $f_{\min}$ as measured on top of a CTF2 doublet.

whether in much quieter condition it will still be true that the effect of water and support structure are not relevant. New measurement campaigns are foreseen to verify these aspects.

6 CONCLUSIONS

Theoretical understanding and experimental results on effect of cooling water on magnet vibrations have been presented. Measurements of the CTF2 quadrupoles have shown that the CLIC tolerances for the vibration of the linac quadrupoles, with nominal water flow, can basically be met. A quadrupole doublet was stabilized at 1.3 nm above 4 Hz, both in vertical and in horizontal directions. The considered CTF2 quadrupoles have the same cross section as the ones foreseen for CLIC, but they are about twenty times shorter. Whether these results can be reproduced for the full scale magnet, is still to be verified. The effect of water pumps needs also to be quantified.

The simplified theory of water induced vibrations gives a reliable rough estimate of the frequency range of the vibrations but is not sufficiently accurate for estimating the RMS amplitude of the motion. Water induced magnet vi-

brations have been proven to be driven by turbulence in the water motion. The main source of quadrupole vibration does not come from the quadrupole pipes but from the pipes feeding the magnet, as is also confirmed by measurement done at SLAC. This is an important issue since the large pipe feeding the quadrupoles induces vibrations in the frequency range of few tens of Hz. In the same frequency range are the structural resonances of the magnets and of their supports. It seems feasible to reduce this effect by adjusting properly the diameter of the feeding pipes, for instance increasing the diameter to concentrate the motion in a frequency range where beam based feedbacks are effective.

The stability of the quadrupole doublet and the effect of water were found to depend considerably on the stabilization device. A stiff system gives the best performance, whilst a soft air pressure system shows an unacceptable amplification of the low frequency vibrations.

7 ACKNOWLEDGMENTS

The authors would like to acknowledge the members of the CLIC Stability Study Group for their support and for helpful discussions and also A. Seyri and H. Braun. G. Yvon and D. Gros did the installation of the water connections. E. Bravin and T. Lefèvre helped for the setup of the measurements in the CTF2 site.

8 REFERENCES

[1] G. Guignard (Ed), *et al.*, *CERN 2000-008*, Geneva (2000).

[2] R. Aßmann *et al.*, "Status of the CLIC Study on Marnet Stabilization and Time-Dependent Luminosity," *EPAC2002*, Paris (2002), also as *CLIC Note* **530**, Geneva (2000).

[3] H.H. Braun, "Experimental Results and Technical Results and Development at CTFII,"*CLIC Note* **441**, Geneva (2000).

[4] W. Coosemans, V.M. Juravlev, G. Ramseier, A.A. Sery, A.I. Sleptsov, I. Wilson, "Investigations of Power and Spatial Correlation Characteristics of Seismic Vibrations in the CERN LEP Tunnel for Linear Collider Studies," *CERN-SL* **93-53** (1993), also in *CLIC Note* **217** (1993).

[5] "Quadrupoles for CLIC Test Facility 2," Tech. Spec. *CERN/AT-MA/95-114/Rev.1*, Geneva (1995).

[6] W. Schnell, "Cooling and Vibration in the CLIC Main Acclerating Structures," *CLIC Note* **468**, Geneva (2001).

[7] L. Landau and E.M. Lifschitz, *Course of Theoretical Physics* Vol. **VI**, (Pergamon Press, London, 1959).

[8] C.F. v. Weiszächer, Z. Physik **124** (1948) p. 614, W. Heisenberg ibid. p. 628.

[9] R. Aßmann, *et al.*, these proceedings.

[10] F. Le Pimpec *et al.*, "Vibrational Stability of NLC Linac Accelerating Structure," *EPAC2002*, Paris (2002).